Supramolecular architecture of new lanthanide coordination polymers of 2-aminoterephthalic acid and 1,10-phenanthroline

Chong-Bo Liu,[ab] Chang-Yan Sun,[a] Lin-Pei Jin*[a] and Shao-Zhe Lu[c]

[a] Department of Chemistry, Beijing Normal University, Beijing 100875, People's Republic of China. E-mail: lpjin@bnu.edu.cn; Fax: +86-10 6220 2075; Tel: +86-10 6220 5522
[b] Department of Chemistry, Nanchang University, Nanchang 330047, People's Republic of China
[c] Laboratory of Excited State Processes, Changchun Institute of Optics, Fine Mechanics and Physics, Chinese Academy of Sciences, Changchun 130021, People's Republic of China

This paper presents five new lanthanide coordination polymers with 2-aminoterephthalic acid (H_2atpt) and 1,10-phenanthroline (phen), [Ln(atpt)$_{1.5}$(phen)(H_2O)]$_n$ [Ln = La (**1**); Eu (**2**)], [Ln$_2$(atpt)$_3$(phen)$_2$(H_2O)]$_n$ [Ln = Tb (**3**); Er (**4**)] and [Yb$_2$(OH)(atpt)$_{2.5}$(phen)$_2$]$_n$·1.75nH$_2$O (**5**), prepared by hydrothermal reactions and structurally characterized. **1** and **2** are isostructural, in which all the Ln^{3+} ions are eight-coordinated. **3** and **4** are also isostructural and have two types of lanthanides; Ln(1) (Ln = Tb, Er) is seven-coordinated and Ln(2) (Ln = Tb, Er) is eight-coordinated in the asymmetric unit. **1**–**4** are two-dimensional rhombus-like grids constructed by bridging atpt ligands, and further form 3-D supramolecular architectures via hydrogen bonds and π–π stacks between phen molecules. Complex **5**, in which there are two eight-coordinated Yb^{3+} ions linked by one hydroxyl group and one atpt ligand in the asymmetric unit, exhibits an interpenetrated 3-D network with a brick structure. In **1**–**4** one atpt ligand is coordinated to three or four Ln^{3+} ions (Ln = La, Eu, Tb, Er) in bridging modes and in **5** one atpt ligand is coordinated to two or three Yb^{3+} ions by double chelating or chelating-bridging mode. The high-resolution emission spectrum of **2** shows only one Eu^{3+} ion site in **2**, which is in agreement with the results of the X-ray diffraction. The thermal stabilities of the supramolecular compounds **2**, **4** and **5** show that the presence of amino groups induces formation of hydrogen bonds that are responsible for the increase in the thermal stability.

Introduction

In recent years, the field of metal-organic coordination polymers has undergone explosive growth in supramolecular and materials chemistry due to the variety of intriguing structural topologies, physico-chemical characteristics, and potential applications as functional materials.[1–4] Especially much attention has been focused on the self-assembly of supramolecular architectures by exploiting non-covalent forces including coordination bonding, hydrogen bonding, aromatic π–π stacking interactions, electrostatic and charge-transfer attractions.[5,6] Supramolecular assembly is a central theme in the design of new solid materials with intriguing structures such as brick wall,[7] square grid,[8] honeycomb,[9] and other geometries.[10–12]

In general, the architectures of such supramolecular networks are built-up using multidentate organic ligands containing O– and/or N– donors, such as polyacids with suitable spacers and 4,4′-bipyridine, to link metal centers to form polymeric structures. For example, the rodlike ligand terephthalic acid (tp) is a good spacer and has been widely used to fabricate large, tightly bound metal cluster aggregates.[13–19] However, much less work has been carried out to investigate coordination polymers of tp derivatives, for example, 2-amino-terephthalic acid (H_2atpt).[20–23] Up to now there have been no systematic studies on lanthanide supramolecular architectures with atpt.

Hydrogen bonds are well suited for the formation of supramolecular structures[24] because they can interlink 1-D or 2-D structures into higher dimensional systems and help in the creation of supramolecular assemblies.[25] The introduction of an amino group to terephthalic acid will contribute to rich hydrogen bonds. On the other hand, π–π stacking is also of fundamental importance for the further development of supramolecular chemistry.[26] Ligands with nitrogen-containing aromatic rings may help supramolecular assembly processes via π–π interactions. It is well known that phen is an appropriate ligand for lanthanide ions and can help to construct stable supramolecular structures via C–H···O or C–H···N hydrogen bonds and π–π stacks.[27] In the present work we selected the La, Eu, Tb, Er, and Yb elements as representatives of light, middle and heavy rare earths, and made use of the hydrothermal technique to obtain five new coordination polymers of lanthanide ions with atpt and phen.

Experimental

General

LaCl$_3$·7H$_2$O, EuCl$_3$·6H$_2$O, TbCl$_3$·6H$_2$O, ErCl$_3$·6H$_2$O, and YbCl$_3$·6H$_2$O were prepared by dissolving their oxides in dilute hydrochloric acid and then evaporating the solvent to dryness. All the other reagents were commercially available and used without further purification. Elemental analyses were performed with an Elementar Vario EL analyzer and IR spectra were measured as KBr discs on a Nicolet Avatar 360 FT-IR spectrometer. Thermogravimetric curves were recorded with a ZRY-2P Thermal Analyzer.

Syntheses

[La(atpt)$_{1.5}$(phen)(H$_2$O)]$_n$ (1). LaCl$_3$·7H$_2$O (0.074 g, 0.2 mmol), 0.055 g H$_2$atpt (0.3 mmol), 0.040 g phen·H$_2$O (0.2 mmol), 10 ml deionized water and 0.6 ml 0.65 M NaOH aqueous solution (0.4 mmol) were sealed in a 25 ml Teflon-lined stainless reactor and heated at 160 °C for 72 h under autogeneous pressure, then cooled at 5 °C h^{-1} to 120 °C, followed by slow cooling to room temperature. The pH of the final solution was 3.5. Light-brown needle-like crystals of **1** were collected by filtration, washed thoroughly with water and ethanol, and air-dried to give 0.045 g of product (36.3%). C$_{24}$H$_{17.5}$LaN$_{3.5}$O$_7$ (605.83): calcd. C 47.58, H 2.91, N 8.09; found C 47.42, H 2.69, N 8.00. IR data (KBr pellet, ν/cm^{-1}): 3466 m, 3339 w, 1618 m, 1572 s, 1515 m, 1493 w, 1430 vs, 1375 vs, 1254 m, 846 m, 774 m, 730 m, 636 w, 557 w, 499 w.

[Eu(atpt)$_{1.5}$(phen)(H$_2$O)]$_n$ (2). EuCl$_3$·6H$_2$O (0.073 g, 0.2 mmol), 0.055 g H$_2$atpt (0.3 mmol), 0.040 g phen·H$_2$O (0.2 mmol), 5 ml deionized water and 0.6 ml 0.65 M NaOH aqueous solution (0.4 mmol) were sealed in a 25 ml Teflon-lined stainless reactor and heated at 160 °C for 72 h under autogeneous pressure, then cooled at 5 °C h^{-1} to 120 °C, followed by slow cooling to room temperature. The pH of the final solution was 3.8. Brown needle-shaped crystals of **2** were obtained, washed with water and ethanol, and air-dried to give 0.052 g of product (42.3%). C$_{24}$H$_{17.5}$EuN$_{3.5}$O$_7$ (618.875): calcd. C 46.57, H 2.85, N 7.92; found C 46.46, H 2.66, N 7.76. IR data (KBr pellet, ν/cm^{-1}): 3463 m, 3342 w, 1631 m, 1617 m, 1575 s, 1517 m, 1495 w, 1433 vs, 1376 vs, 1255 m, 847 m, 773 m, 731 m, 637 w, 562 w, 510 w.

[Ln$_2$(atpt)$_3$(phen)$_2$(H$_2$O)]$_n$ [Ln = Tb (3), Er (4)]. The syntheses of complexes **3** and **4** followed the same procedure as for **1**. The final solution pHs of **3** and **4** were 3.6 and 3.5, respectively. Tiny light yellow crystals of **3** and **4** were obtained by filtration, washed thoroughly with water and ethanol, and air-dried to give yields of 38.4% (0.048 g) and 43.2% (0.054 g), respectively. C$_{48}$H$_{33}$Tb$_2$N$_7$O$_{14}$ (**3**; 1233.65): calcd. C 46.73, H 2.70, N 7.95; found C 46.63, H 2.47, N 7.62. IR data (KBr pellet, ν/cm^{-1}): 3449 m, 3340 w, 1634 m, 1618 m, 1575 s, 1517 m, 1496 w, 1433 vs, 1375 vs, 1254 m, 848 m, 775 m, 731 m, 638 w, 562 w, 509 w. C$_{48}$H$_{33}$Er$_2$N$_7$O$_{14}$ (**4**; 1250.33): calcd. C 46.11, H 2.66, N 7.84; found C 45.89, H 2.45, N 7.75. IR data (KBr pellet, ν/cm^{-1}): 3447 m, 3338 w, 1639 m, 1617 m, 1576 s, 1517 m, 1496 w, 1434 vs, 1374 vs, 1253 m, 848 m, 775 m. 731 m, 638 w, 562 w, 516 w.

[Yb$_2$(OH)(atpt)$_{2.5}$(phen)$_2$]$_n$·1.75nH$_2$O (5). The synthesis of complex **5** followed the same procedure as for **2**. The final solution pH of **5** was 4.1. Tiny light yellow crystals of **5** were obtained by filtration, washed thoroughly with water and ethanol, and air-dried to give 0.032 g of product (26.67%). C$_{44}$H$_{33}$Yb$_2$N$_{6.5}$O$_{12.25}$ (1202.85): calcd. C 43.93, H 2.77, N 7.57; found C 43.89, H 2.57, N 7.41. IR data (KBr pellet, ν/cm^{-1}): 3438 m, 3336 w, 2918 w, 1625 w, 1541 s, 1425 vs, 1387 vs, 1334 m, 1260 m, 852 m, 772 m, 726 m, 637 w, 561 w.

Measurement of the high-resolution luminescence spectra

The excitation light source was a YAG: Nd laser using the excitation wavelength at 355 nm. The sample was placed in a Dewar's bottle and cooled with liquid nitrogen. The fluorescence was collected at right angles through a Spex 1403 monochromator with a photomultiplier tube, then averaged by a boxcar integrator and finally the data were transferred to a computer.

X-Ray crystallographic study

The X-ray single-crystal data of **1**, **2**, **3**, **4**, and **5** were collected using a Bruker SMART 1000 CCD area detector diffractometer with graphite-monochromated MoKa radiation ($\lambda = 0.71073$ Å). Semi-empirical absorption corrections were applied to all five complexes using the SADABS program. The structures were solved by direct methods and refined by full-matrix least squares on F^2 using SHELXL 97.[28] All non-hydrogen atoms were refined anisotropically. Hydrogen atoms were placed in geometrically calculated positions.†

Results and discussion

Crystallographic study

Crystal data of the title complexes are listed in Table 1 and selected bond lengths of **1**–**5** are listed in Table 2. The H$_2$atpt ligands are all completely deprotonated and engage in six types of coordination modes, shown as a–f in Scheme 1. X-Ray single crystal diffraction studies reveal that **1** and **2**, **3** and **4** are isostructural, respectively. So only the structures of **2**, **4**, and **5** will be discussed in detail.

[Eu(atpt)$_{1.5}$(phen)(H$_2$O)]$_n$ (2). The asymmetric unit of **2** consists of one europium(III) ion, which is coordinated to eight atoms: five carboxylate oxygen atoms [O(1), O(5), O(3a), O(4a), O(6a)] from five atpt ligands, one oxygen atom [O(7)] from a water molecule and two nitrogen atoms [N(1), N(2)] from a chelating phen molecule (Fig. 1). There are three coordination modes for the carboxylate groups of atpt ligands in **2**: (a) both of the carboxylate groups of an atpt ligand adopt a bridging bidentate mode [Scheme 1(a)]; (b) the carboxylate group adjacent to the amino group adopts a bridging bidentate mode, while the other adopts a monodentate mode, leaving one oxygen atom uncoordinated [Scheme 1(b)]; (c) the carboxylate group adjacent to the amino group adopts a monodentate mode, but the other one adopts a bridging bidentate mode [Scheme 1(c)]. So, each atpt ligand links three or four europium atoms and each Eu(III) ion is attached to five atpt ligands.

The building block contains two europium ions. The distance between the two Eu(III) ions is 4.137 Å. The two Eu(III) ions in one building block are bridged by carboxylate groups of atpt anions [see Scheme 1(a–c)]. Along the *a* axis, every two blocks are joined by a tetradentate atpt ligand; while along the *b* axis, every two blocks are joined by two tridentate atpt ligands, giving rise to a 2-D layer structure containing a regular rhomboid grid with dimensions of 10.87×11.61 Å^2 based on the Eu···Eu distance (see Fig. 2).

In fact all the Eu(III) ions of this layer structure occupy two perfect parallel planes with a mean deviation of 0.0 Å, as shown in Scheme 2. All the phen molecules of this layer structure are distributed in two perfect parallel planes, too. The dihedral angle between the planes of phen molecules and those of Eu(III) ions is 70.8°.

There are abundant hydrogen bonds in **2**, which play an important role in supramolecular assembly. The hydrogen bonds are formed: (a) between coordinated water molecules and uncoordinated carboxylate oxygen atoms; (b) between the amino group and uncoordinated carboxylate oxygen atoms; (c) between the amino group and coordinated carboxylate oxygen atoms; (d) between the coordinated carboxylate oxygen atoms and C–H of phen molecules; (e) between the nitrogen atoms of amino groups and C–H of phen molecules, as shown in Table 3. The average distance between two phen

---

† CCDC reference numbers 222 296–222 300. See http://www.rsc.org/suppdata/nj/b4/b402803a/ for crystallographic data in .cif or other electronic format.

Table 1 Crystal data for **1**, **2**, **3**, **4** and **5**

Complex	1	2	3	4	5
Empirical formula	$C_{24}H_{17.5}N_{3.5}O_7La$	$C_{24}H_{17.5}N_{3.5}O_7Eu$	$C_{48}H_{33}N_7O_{13}Tb_2$	$C_{48}H_{33}N_7O_{13}Er_2$	$C_{44}H_{33}N_{6.5}O_{12.75}Yb_2$
Formula weight	605.83	618.875	1233.65	1250.33	1202.85
T/K	293(2)	293(2)	293(2)	293(2)	293(2)
Crystal system	Triclinic	Triclinic	Triclinic	Triclinic	Monoclinic
Space group	$P\bar{1}$	$P\bar{1}$	$P\bar{1}$	$P\bar{1}$	$P2_1/c$
a/Å	10.6876(9)	10.497(3)	10.518(3)	10.4948(16)	12.998(3)
b/Å	11.0638(8)	10.870(3)	11.091(4)	11.0961(10)	15.816(3)
c/Å	11.4747(9)	11.355(3)	19.544(6)	19.497(2)	21.168(5)
α/deg	69.080(6)	70.836(4)	73.846(4)	73.554(7)	90
β/deg	87.883(6)	87.853(4)	85.663(5)	85.545(8)	106.996(10)
γ/deg	65.576(6)	65.793(4)	84.416(5)	84.474(8)	90
U/Å³	1144.15(16)	1109.1(6)	2176.7(12)	2164.4(5)	4161.7(15)
Z	2	2	2	2	4
μ/mm⁻¹	1.920	2.882	3.302	3.930	4.543
No. data collected	5495	6414	11 225	9661	16 441
No. unique data	3926	4488	7494	7400	8241
R_{int}	0.0264	0.0282	0.0330	0.0448	0.0567
$R_1 [I > 2\sigma(I)]$	0.0336	0.0330	0.0347	0.0461	0.0431
wR_2 (all data)	0.0701	0.0714	0.0625	0.0836	0.0901

Table 2 Selected bond lengths^a (Å) for **1–5**

1

La(1)–O(1)	2.446(3)	La(1)–O(6)#2	2.501(3)
La(1)–O(3)#3	2.526(3)	La(1)–O(7)	2.576(3)
La(1)–O(4)#1	2.495(3)	La(1)–N(1)	2.733(4)
La(1)–O(5)	2.415(3)	La(1)–N(2)	2.719(4)

2

Eu(1)–O(1)	2.330(3)	Eu(1)–O(6)#4	2.311(3)
Eu(1)–O(3)#5	2.354(3)	Eu(1)–O(7)	2.498(3)
Eu(1)–O(4)#6	2.399(3)	Eu(1)–N(1)	2.649(4)
Eu(1)–O(5)	2.394(3)	Eu(1)–N(2)	2.601(4)

3

Tb(1)–O(1)	2.279(4)	Tb(2)–O(2)	2.368(4)
Tb(1)–O(3)#1	2.226(4)	Tb(2)–O(5)	2.373(4)
Tb(1)–O(6)	2.352(4)	Tb(2)–O(7)#7	2.311(4)
Tb(1)–O(10)	2.309(4)	Tb(2)–O(9)	2.391(4)
Tb(1)–O(12)	2.323(4)	Tb(2)–O(11)	2.313(4)
Tb(1)–N(1)	2.571(5)	Tb(2)–O(13)	2.406(4)
Tb(1)–N(2)	2.585(5)	Tb(2)–N(3)	2.612(5)
		Tb(2)–N(4)	2.560(5)

4

Er(1)–O(1)	2.231(6)	Er(2)–O(2)	2.327(6)
Er(1)–O(3)#1	2.184(6)	Er(2)–O(5)	2.323(6)
Er(1)–O(6)	2.291(6)	Er(2)–O(7)#7	2.273(6)
Er(1)–O(10)	2.264(6)	Er(2)–O(9)	2.353(6)
Er(1)–O(12)	2.290(6)	Er(2)–O(11)	2.290(6)
Er(1)–N(1)	2.547(8)	Er(2)–O(13)	2.392(5)
Er(1)–N(2)	2.562(7)	Er(2)–N(3)	2.587(7)
		Er(2)–N(4)	2.525(8)

5

|			
Yb(1)–O(1)	2.396(5)	Yb(2)–O(3)#9	2.376(5)
Yb(1)–O(2)	2.356(5)	Yb(2)–O(4)#9	2.376(5)
Yb(1)–O(8)#8	2.226(5)	Yb(2)–O(5)	2.435(6)
Yb(1)–O(9)	2.342(6)	Yb(2)–O(6)	2.317(5)
Yb(1)–O(10)	2.352(5)	Yb(2)–O(7)#8	2.297(6)
Yb(1)–O(11)	2.231(5)	Yb(2)–O(11)	2.213(4)
Yb(1)–N(1)	2.472(7)	Yb(2)–N(3)	2.498(7)
Yb(1)–N(2)	2.513(6)	Yb(2)–N(4)	2.445(7)

^{a} Symmetry operation: #1 $-x+1, -y+2, -z$; #2 $-x+2, -y+1, -z$; #3 $x+1, y-1, z$; #4 $-x+1, -y+1, -z+1$; #5 $-x+2, -y, -z+1$; #6 $x-1, y+1, z$; #7 $-x+2, -y+1, -z+1$; #8 $-x, y-1/2, -z+1/2$; #9 $x-1, -y+3/2, z-1/2$.

planes in the same grid is 3.6 Å and that between two phen planes of adjacent layers is 3.4 Å. Therefore, two kinds of π–π aromatic interactions exist among the phen molecules. It is these rich hydrogen bonds and π–π stacks between phen molecules that generate the 3-D supramolecular structure.

$[Er_2(atpt)_3(phen)_2(H_2O)]_n$ (4). Complex **4** is composed of the dinuclear species $[Er_2(atpt)_3(phen)_2(H_2O)]$ with an Er(1)··· Er(2) distance of 4.15 Å. The Er(1) atom is seven-coordinated to two nitrogen atoms from a chelating phen molecule and five oxygen atoms from five separate atpt ligands; the Er(2) atom is eight-coordinated with five oxygen atoms belonging to five atpt ligands, another one from one coordinated water molecule, with the last two coordination sites being occupied by two nitrogen atoms from a chelating phen molecule, as shown in Fig. 3. The coordination modes of atpt ligands are the same as those of **2**.

Every asymmetric unit $[Er_2(atpt)_3(phen)_2(H_2O)]$ is a building block and is bridged by six atpt ligands linking four adjacent asymmetric units, which results in a 2-D layer structure parallel to the *ac* plane. The 2-D layer structure has an infinite rhombus grid with dimensions of *ca.* 11.40×10.9 Å² based on the Er···Er distance. The Er(III) ions in this 2-D structure are not coplanar but distributed in two parallel planes, which both have an average atomic displacement of 0.078 Å; the distance between the two planes is *ca.* 3.55 Å. The dihedral angle between the phen molecule planes in this 2-D layer structure is 2.4°, different from that in **2**. This may arise from the facts that there are two different coordination environments of Er(III) ions in **4** and the dihedral angle between phen molecule and Er(III) ion planes are *ca.* 69.2° and 68.2°, respectively. The average distance between two phen planes in the same grid is 3.3 Å and that between two phen planes of adjacent layers is 3.5 Å, which construct a stable 3-D supramolecular network in combination with abundant hydrogen bonds in **4**, as shown in Table 3.

$[Yb_2(OH)(atpt)_{2.5}(phen)_2]_n \cdot 1.75nH_2O$ (5). As shown in Fig. 4, there are two crystallographically independent Yb(III) ions separated by a distance of 4.137 Å, which are linked by a μ₂-bridging hydroxyl group and a bridging bidentate carboxylate of an atpt ligand in an asymmetric unit (Fig. 4). Each Yb³⁺ ion lies in a distorted square anti-prism and is coordinated to two nitrogen atoms from phen, one oxygen atom from a μ₂-bridging hydroxyl group, and five oxygen atoms
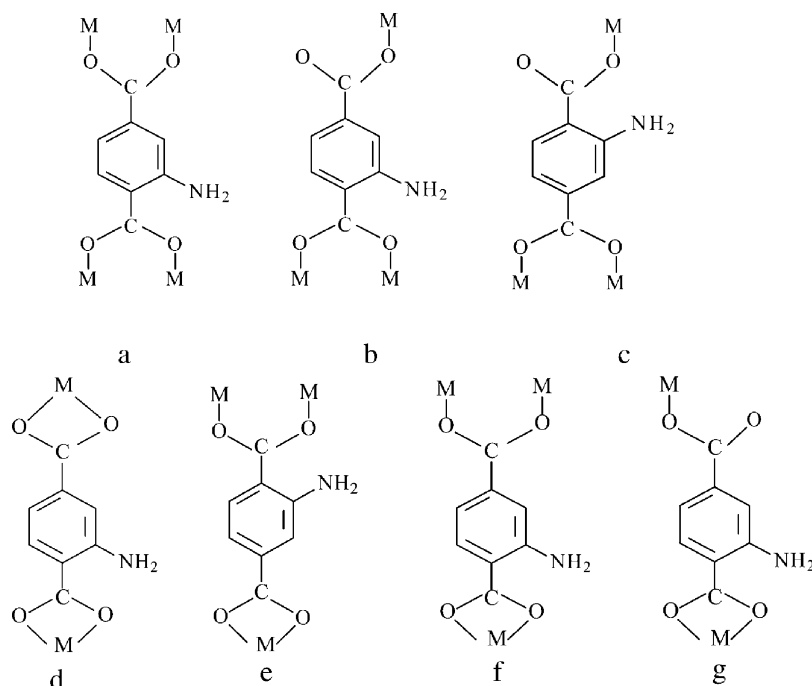
Scheme 1 The seven crystallographically established coordination modes of the atpt ligand.

from three atpt ligands. The coordination environments of Yb(1) and Yb(2) are similar, but the bond lengths of Yb(1)–O and Yb(2)–O, Yb(1)–N and Yb(2)–N are different. For the Yb(1) atom, the Yb(1)–O distances are in the range of 2.226(5)–2.396(5) Å, the Yb(1)–N distances are 2.472(7) and 2.513(6) Å while for the Yb(2) atom, the Yb(2)–O distances ranges from 2.213(4) to 2.435(6) Å, the Yb(2)–N distances are 2.445(7) and 2.498(7) Å. There are three coordination modes for atpt ligands in **5**, which are different from those in **1–4**: (a) the two carboxylate groups of the atpt ligand are coordinated to two Yb(III) ions of different dimeric units in a chelating coordination mode [Scheme 1(d)]; (b) the carboxylate group adjacent to the amino group of atpt connects two Yb(III) ions of the same dimeric unit *via* a bridging bidentate mode while the other one is chelated to one Yb(III) ion of another dimeric unit [Scheme 1(e)]; (c) as shown in Scheme 1(f), the carboxylate group adjacent to the amino group of atpt is

coordinated to one Yb(III) ion in a chelating mode while the other one links two Yb(III) ions in a bridging bidentate mode. So, one atpt ligand links two or three Yb(III) ions and each Yb(III) ion is attached to three atpt ligands.
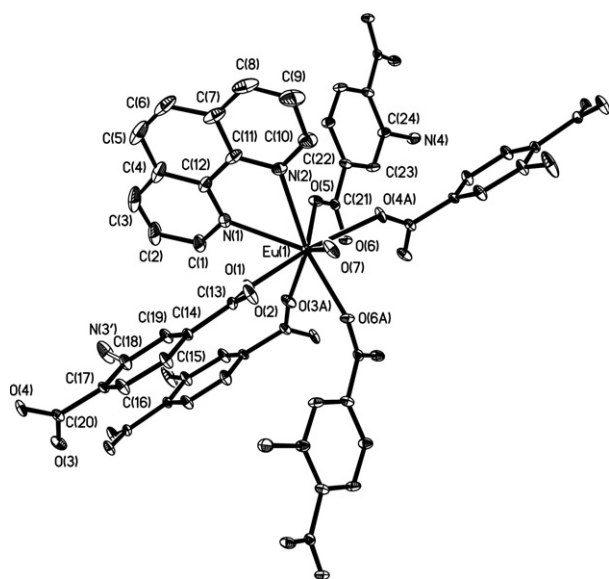

Fig. 2 Packing diagram of [Eu(atpt)$_{1.5}$(phen)(H$_2$O)]$_n$ along the *c* axis. Carbon atoms of phen molecules and all the hydrogen atoms are omitted for clarity.

Fig. 1 Asymmetric unit of [Eu(atpt)$_{1.5}$(phen)(H$_2$O)]$_n$ with 20% thermal ellipsoids. All the hydrogen atoms are omitted for clarity.
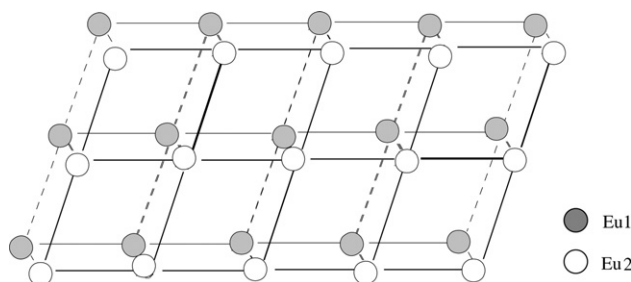
Scheme 2 The metal-organic framework model of the 2-D layer in [Eu(atpt)$_{1.5}$(phen)(H$_2$O)]$_n$.

Table 3 Types of hydrogen bond in **1**–**5**

Complex	Types of hydrogen bonds[a]				
1 and **2**	O_{W1}–H$\cdots$$O_{C1}$	N–H$\cdots$$O_{C1}$	N–H$\cdots$$O_{C2}$	C–H$\cdots$$O_{C2}$	C–H$\cdots$N
3 and **4**	O_{W1}–H$\cdots$$O_{C1}$	N–H$\cdots$$O_{C1}$	N–H$\cdots$$O_{C2}$	C–H$\cdots$$O_{C2}$	C–H$\cdots$N	N–H$\cdots$$\pi$
5	N–H$\cdots$N	N–H$\cdots$$O_{W2}$	N–H$\cdots$$O_{C2}$	C–H$\cdots$$O_{W2}$	C–H$\cdots$N

[a] Atoms are labelled as follows: O_{C1}: the uncoordinated carboxylate oxygen atom; O_{C2}: the coordinated carboxylate oxygen atom; O_{W1}: the oxygen atom of the coordinated water molecule; O_{W2}: the oxygen atom of lattice water molecule; N: the nitrogen atom of the amino group; C: the carbon atom of phen.

The complicated 3-D framework structure of **5** is constructed from the dinuclear $[Yb_2(OH)(atpt)_{2.5}(phen)_2]$ species. Firstly, the O(11) atom of the hydroxyl group links two Yb^{3+} ions of one dinuclear subunit, the angle Yb(1)–O(11)–Yb(2) being 137.1°; then every two Yb_2 subunits are linked together *via* the long bridges of atpt ligands [Scheme 1(d)] to form a chain. As shown in Fig. 5, Yb(2I), Yb(1B), Yb(2B), Yb(1J) and Yb(2L) form chain 1; Yb(2F), Yb(1F), Yb(2G), Yb(1G), Yb(2D) and Yb(1D) form chain 2; similarly, Yb(1C), Yb(2C), Yb(1H), Yb(2H), Yb(1A) and Yb(2A), chain 3, and Yb(2K), Yb(1I), Yb(2E), Yb(1E) and Yb(2J), chain 4. Chains 1, 2, 3 and 4 are nearly parallel to each other. The distances between adjacent Yb(1), Yb(1) and Yb(2), Yb(2) pairs in the same chain are 15.164 and 14.175 Å, respectively, Yb(2) ions of chain 1 are connected with Yb(2) ions of chain 2 by atpt ligands and similarly, Yb(2) ions of chain 3 are connected with Yb(2) ions of chain 4 by atpt ligands [Scheme 1(e or f)], which form a regular parallelogram grid with *ca.* 14.175×11.413 Å^2 dimensions based on the Yb$\cdots$Yb distance. Moreover, Yb(1F) and Yb(1D) of chain 2 are linked with Yb(1C) and Yb(1A) of chain 3 by one atpt ligand [Scheme 1(d)], forming a larger parallelogram grid that is divided into two smaller parallelogram grids of *ca.* 15.164×11.117 Å^2 size, based on the Yb$\cdots$Yb distance, by two atpt ligands. So the structure consists of two grids with different sizes, which can be viewed as a 2-D "brick" layer structure. These layers are further connected by long bridges of atpt ligands to generate the final 3-D framework.

It should be noted that the actual crystal structure of **5** is an interpenetrating 3-D coordination framework with shrunken channels filled by phen and uncoordinated water, owing to steric hindrance effects and electrostatic interactions. The types of hydrogen bonds in **5** are given in Table 3.
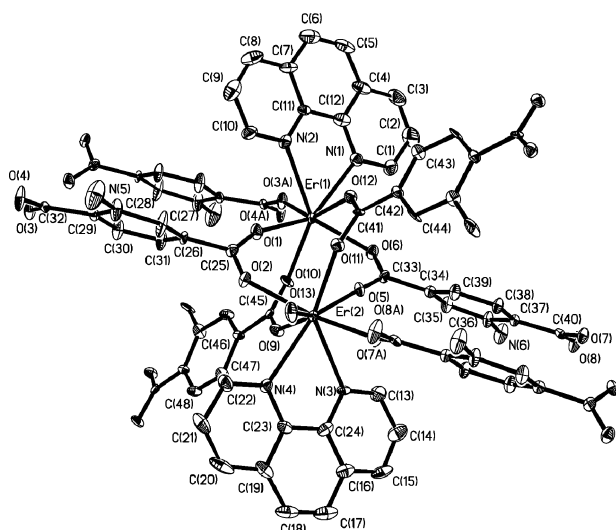
Comparison of X-ray structures. Interestingly, the pH values of the final solutions of **1**–**5** are similar. For example, the reaction conditions of **2** and **5** are the same and the final pH values of **2** and **5** are 3.8 and 4.1, respectively, but their structures are completely different. In **5** hydroxyl groups bridge Yb^{3+} ions while in **1**–**4** water molecules are coordinated to Ln(III) ions directly. To try to obtain the bridging hydroxyl group in **2**, more base was added to the mixture so that the pH value of the final solution in **2** was 4.1 which is the same as that of **5**. The elemental analysis results indicate that the composition of the crystal is the same as that of **2** obtained at a final pH 3.8, which might result from the fact that the Yb(III) complex is easier to hydrolyze than the Eu(III) complex under hydrothermal condition.

In terms of the structural characteristics and the formation of the supramolecular architecture of the title complexes, some remarks can be made. (1) **1**–**4** own their 3-D supramolecular structure to hydrogen bonds and π–π stacks between phen molecules. Each complex has one coordinated water molecule to meet the high coordination number of Ln(III) ions. **5** exhibits a 3-D structure formed through coordination bonds and one hydroxyl group in place of one water molecule coordinates to two Yb(III) ions while water molecules exist in the lattice *via* hydrogen bonds. (2) There are only two types of hydrogen bonds (O–H$\cdots$O and C–H$\cdots$O) in $[Eu(tp)_{1.5}(phen)(H_2O)]_n$ and $[Yb_2(tp)_3(phen)_2(H_2O)]_n$ (tp = terephthalic acid);[29] introduction of the amino group to tp brings rich hydrogen bonds to **1-5**. In addition to O–H$\cdots$O and C–H$\cdots$O hydrogen bonds,

Fig. 3 Asymmetric unit of $[Er_2(atpt)_3(phen)_2(H_2O)]_n$ with 20% thermal ellipsoids. All the hydrogen atoms are omitted for clarity.
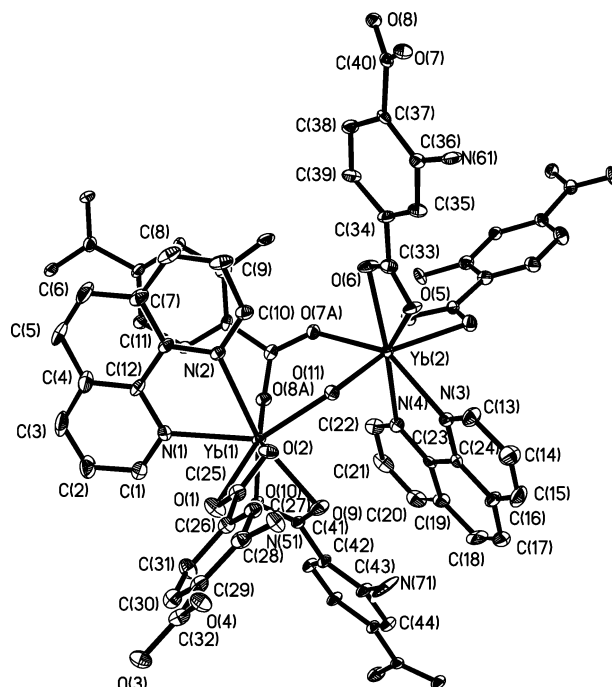

Fig. 4 Asymmetric unit of $[Yb_2(OH)(atpt)_{2.5}(phen)_2]_n \cdot 1.75nH_2O$ with 20% thermal ellipsoids. All the hydrogen atoms are omitted for clarity.

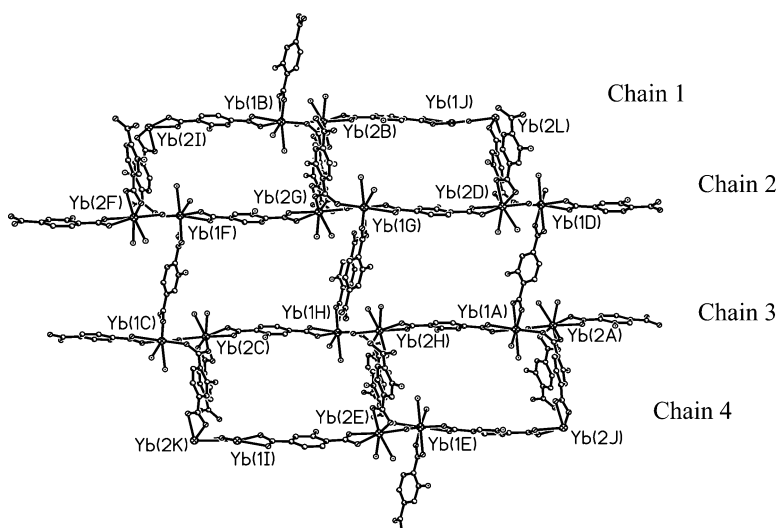**Fig. 5** One layer of the $[Yb_2(OH)(atpt)_{2.5}(phen)_2]_n \cdot 1.75nH_2O$ packing diagram. Carbon atoms of phen molecules and all the hydrogen atoms and lattice water molecules are omitted for clarity.

there are N–H$\cdots$O, N–H$\cdots$N, C–H$\cdots$N, and N–H$\cdots\pi$ hydrogen bonds in **1**–**5**. (3) In **1**–**4** there are two kinds of π–π stacks, one between phen molecules in the same 2-D layer, another between phen molecules of adjacent layers. (4) In **1**–**4** the average bond length of Ln–O$_{carboxylate}$ is shorter than that of Ln–O$_w$, while in **5** the average bond length of Yb–O$_{carboxylate}$ is longer than that of Yb–O$_{OH}$. This is because of the change of coordination mode. Both the average bond lengths of Ln–O, Ln–N and the coordination numbers of the Ln(III) ions show the lanthanide contraction effect in the series on the whole, as shown in Table 4.

There are plentiful coordination modes for the atpt ligand in the title complexes. (1) Comparing with the transition metal complexes of atpt, in [Co(atpt){1,2-bis(4-pyridyl)ethane}]$_n$ one carboxylate group of an atpt ligand chelates to one metal ion while the other links one metal ion in a monodentate mode, as shown in Scheme 1(g).[21] In Zn(atpt)(DMF)(C$_6$H$_5$Cl)$_{0.25}$ one atpt ligand is bonded to four zinc atoms in a bis-bidentate fashion, as shown in Scheme 1(a).[20,30] In the above reported d block transition metal complexes the atpt ligand adopts only one bridging mode. However, in the title complexes atpt adopts three different bridging modes in every complex. This can be attributed to the larger radii and greater positive charge of Ln(III) ions, and hence large coordination numbers and different coordination modes are required by lanthanide ions. (2) As regards the atpt ligand, two coordination modes [Scheme 1(e,f)] are not present in the binary lanthanide complexes.[22,23] In the ternary lanthanide complexes with tp and phen,[29] tp adopts μ_3-bridging and μ_4-bridging modes; double chelating and chelating-bridging modes [Scheme 1(d–f)] are not present.

All the reported binary lanthanide complexes with tp[17–19] or atpt[22,23] are 3-D networks sustained by coordination bonds. The introduction of phen may lead to lower dimensionality of coordination, owing to one phen occupying two coordination sites by adopting chelating mode; however, it can be found that phen has an important effect on the construction of supramolecular structures, which may be of high interest for the design of advanced supramolecular materials.

Photophysical properties of $[Eu(atpt)_{1.5}(phen)(H_2O)]_n$

Emission spectra and emission lifetimes were measured for the excitation at 355 nm at 293 and 77 K. Emission spectra of **2** are shown in Fig. 6. It is well-known that the $^5D_0 \rightarrow {}^7F_2$ transition induced by the electric dipole moment is hypersensitive to the coordination environment of the Eu(III) ion, while the $^5D_0 \rightarrow {}^7F_1$ transition is a magnetic dipole one, which is fairly insensitive to the environment of the Eu(III) ion. The intensity ratio $I (^5D_0 \rightarrow {}^7F_2/^5D_0 \rightarrow {}^7F_1)$ is equal to 6.12, which indicates that the Eu(III) ion is not located at a center of inversion and
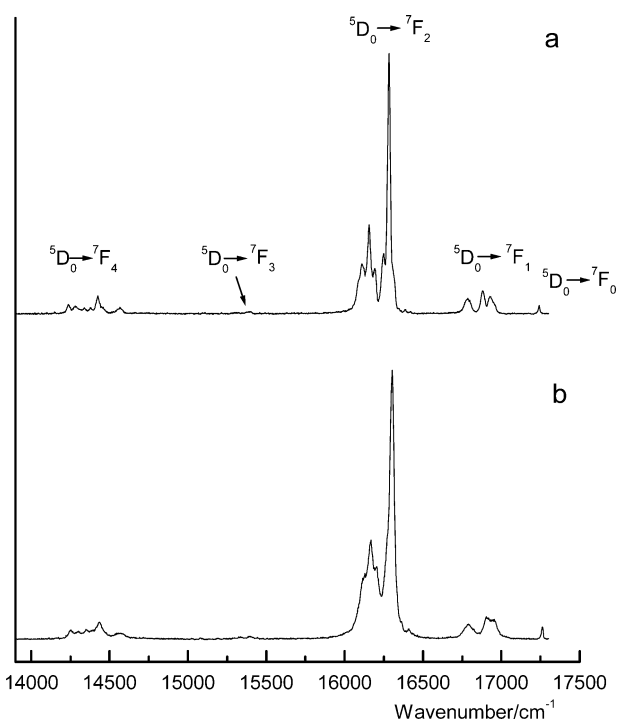
Table 4 The average bond lengths and the coordination number (CN) in **1**–**5**

Complex	CN	Ln–O(carboxylate)	Ln–O(water or OH)	Ln–N
1	8	2.4766	2.576	2.726
2	8	2.3576	2.498	2.625
3	7, 8	2.3245	2.406	2.582
4	7, 8	2.2826	2.392	2.555
5	8	2.3472	2.222	2.482

Average bond length/Å

Fig. 6 Emission spectra of **2** corresponding to the $^5D_0 \rightarrow {}^7F_J$ ($J = 0$–4) transitions ($\lambda_{exc} = 355$ nm): (a) 77 K and (b) 293 K.

that the symmetry of the Eu(III) ion site is low.[31] This is in agreement with the result of the single-crystal X-ray analysis. From Fig. 6 it can be seen that emission bands are at $17\,242$ cm^{-1} ($^5D_0 \rightarrow {}^7F_0$), 16 928, 16 880 and 16 786 cm^{-1} ($^5D_0 \rightarrow {}^7F_1$) and 16 282, 16 248, 16 192, 16 156 and 16 110 cm^{-1} ($^5D_0 \rightarrow {}^7F_2$) at 77 K while they are at 17 262 cm^{-1} ($^5D_0 \rightarrow {}^7F_0$), 16 946, 16 916 and 16 796 ($^5D_0 \rightarrow {}^7F_1$) and 16 304, 16 262 (shoulder), 16 202, 16 168 and 16 124 cm^{-1} at 293 K.$^5D_0 \rightarrow {}^7F_3$ emission bands are very weak and $^5D_0 \rightarrow {}^7F_4$ emission bands are overlapped, effects that are not discussed here. Comparing the emission spectrum of **2** at 77 K with that at 293 K, the low-temperature spectrum shows the expected bathochromic shift and line narrowing.

Decay curves of **2** are shown in Fig. 7. Luminescence lifetimes of **2** are 533 µs at 293 K and 688 µs at 77 K. This can be explained by considering the fact that the coordinated water molecules partially quench the luminescence and decrease the τ value through vibronic coupling with the vibrational states of the O–H oscillators; very efficient nonradiative deactivation takes place in the europium excited state at higher temperature.[32]

Fig. 8 is the time-resolved spectra measured at different delay times. From Fig. 8 it can be seen that no significant changes in intensity, position and shape of emission bands was observed as the delay time was varied; the $2J+1$ components of the $^5D_0 \rightarrow {}^7F_J$ ($J = 0$, 1, 2) transitions (also see Fig. 6) were obtained, displaying a single Eu(III) ion site in **2**.[31] The results show that the Eu(III) ion is a sensitive luminescence probe for the Eu^{3+} site in europium coordination polymers.

Thermogravimetric analyses

The presence of the water molecules is confirmed by thermogravimetric analyses of complexes **2**, **4**, and **5**. For **2**, the first weight loss of 2.8% from 215 °C to 276 °C corresponds to the loss of two coordinated water molecules per dinuclear unit (calcd 2.91%). Increasing temperature leads to the further decomposition of **2** at 380 °C and the final pyrolysis was completed at 754 °C, as indicated by a significant weight loss 68.1%; Eu$_2$O$_3$ (calcd. 68.6%) was obtained. For **4**, the first weight loss of 1.33% from 255 °C to 299 °C corresponds to the loss of one coordinated water molecule per dinuclear unit (calcd. 1.44%). Further decomposition of **4** occurred above 406 °C and was completed at 840 °C, giving a powder of Er$_2$O$_3$ (found 68.9%, calcd. 69.4%). The TGA curve of **5** shows that the first weight loss of 2.45%, which occurred at 138 °C and ended at 196 °C, corresponds to the loss of one and
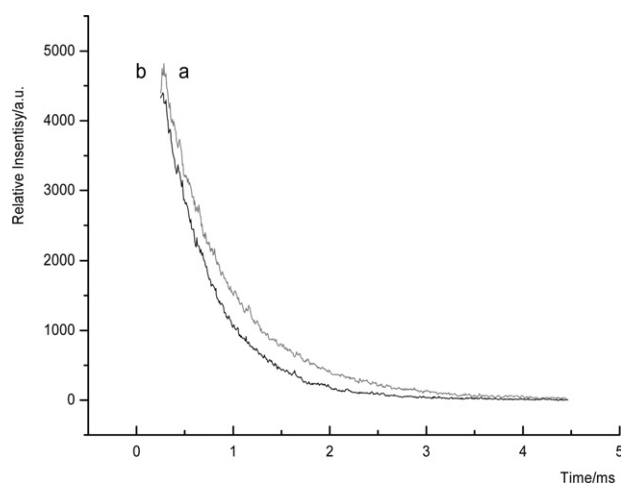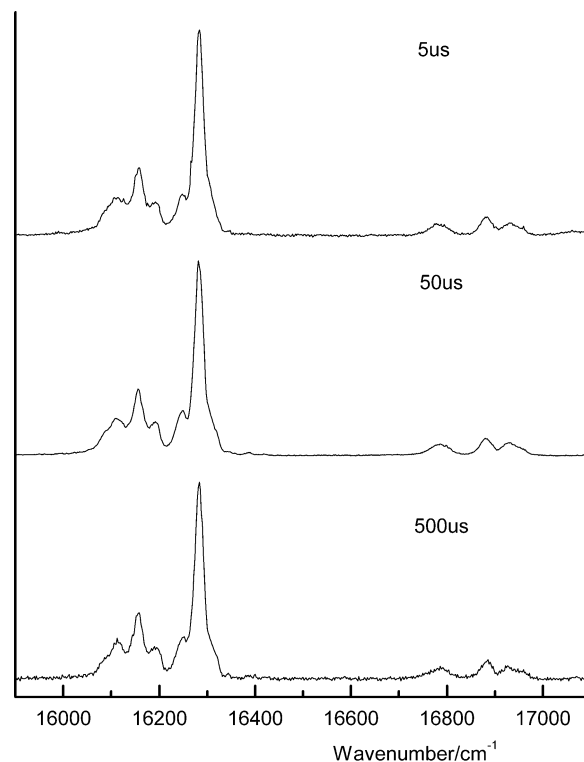

Fig. 8 Time-resolved spectra of **2** at 77 K in the range of 15 900–17 100 cm^{-1}; delay times: 5, 50, 500 µs; $\lambda_{exc} = 355$ nm.

three-fourths lattice water molecules per subunit (calcd: 2.62%). Further decomposition occurred above 475 °C and the final pyrolysis ended at 864 °C, as indicated by a significant weight loss 64.2%; Yb$_2$O$_3$ (calcd. 64.6%) was obtained.

The TGA curves of **2**, **4**, and **5** show that the dehydration temperature of **5** is much lower than that of **2** or **4**, which is in line with the lattice water in **5**, and the ending decomposition temperature of **5** is higher than that of **2** or **4**, which is consistent with the fact that the metal-organic framework can be stabilized by interpenetrating lattices.[11,33] The dehydration temperatures of **2**, **4** and **5** are far higher than that of complex [Er$_4$(tp)$_6$·6H$_2$O]$_n$ (90–133 °C)[19] and that of complex [Er$_2$(atpt)$_3$·5.5H$_2$O]$_n$ (50–160 °C),[23] which suggests that the introduction of the amino group to tp and phen helps to increase thermal stability, which may be due to rich hydrogen bonds and π–π stacking.

Fig. 7 Decay curves of **2**: (a) 77 K, $\nu_{anal} = 16\,285$ cm^{-1}; (b) 293 K, $\nu_{anal} = 16\,303$ cm^{-1}.

Conclusion

The first examples of lanthanide supramolecular complexes with two different organic ligands, atpt and phen, have been obtained and characterized by X-ray crystallography. All compounds are very stable in air at ambient temperature and almost insoluble in common solvents such as water, alcohol and acetone. The atpt ligands in these complexes adopt tridentate and tetradentate coordination modes to coordinate with Ln(III) ions. IR spectra show that the carboxylate groups are completely deprotonated because there is no strong absorption from 1720 to 1680 cm^{-1}. Hydrogen bonds and π–π stacking clearly contribute to the formation of 3-D supramolecular structures in the title complexes. The lifetime of the Eu(III) ion in **2** is shortened because of the presence of coordinated water molecules and amino group in the europium complex. However, introduction of the amino group into the benzene ring leads to formation of hydrogen bonds, which increases the thermal stability of the complexes.

Acknowledgements

References

1 O. M. Yaghi, H. Li, C. Davis, D. Richardson and T. L. Groy, *Acc. Chem. Res.*, 1998, **31**, 474.
2 M. Eddaoudi, D. B. Moler, H. Li, B. Chen, T. M. Reineke, M. O'Keeffe and O. M. Yaghi, *Acc. Chem. Res.*, 2001, **34**, 319.
3 T. M. Reineke, M. Eddaoudi, M. O'Keeffe and O. M. Yaghi, *Angew. Chem., Int. Ed.*, 1999, **38**, 2590.
4 G. Seward, N.-X. Hu and S. Wang, *J. Chem. Soc., Dalton Trans.*, 2001, 134.
5 B. Moulton and M. J. Zaworotko, *Chem. Res.*, 2001, **101**, 1629.
6 J.-M. Lehn, *Angew. Chem., Int. Ed. Engl.*, 1988, **27**, 89.
7 M. Fujita, Y. J. Kwon, O. Sasaki, K. Yamaguchi and K. Ogura, *J. Am. Chem. Soc.*, 1995, **117**, 7287.
8 M. Fujita, Y. J. Kwon, S. Washizu and K. Ogura, *J. Am. Chem. Soc.*, 1994, **116**, 1151.
9 G. B. Gardner, D. Venkataraman, J. S. Moore and S. Lee, *Nature (London)*, 1995, **374**, 792.
10 D. Sun, R. Cao, Y. Liang, Q. Shi, W. Su and M. Hong, *J. Chem. Soc., Dalton Trans.*, 2001, 2335.
11 J.-C. Dai, X.-T. Wu, Z.-Y. Fu, S.-M. Hu, W.-X. Du, C.-P. Cui, L.-M. Wu, H.-H. Zhang and R.-Q. Sun, *Chem. Commun.*, 2002, 12.
12 B. F. Hoskins and R. Robson, *J. Am. Chem. Soc.*, 1990, **112**, 1546.
13 M. Eddaoudi, J. Kim, N. Rosi, D. Vodak, J. Wachter, M. O'Keeffe and O. M. Yaghi, *Science*, 2002, **295**, 469.
14 J. S. Seo, D. Whang, H. Lee, S. I. Jun, J. Oh, Y. J. Jeon and K. Kim, *Nature (London)*, 2000, **404**, 982.
15 H. Li, C. E. Davis, T. L. Groy, D. G. Kelley and O. M. Yaghi, *J. Am. Chem. Soc.*, 1998, **120**, 2186.
16 K. Seki and W. Mori, *J. Phys. Chem. B.*, 2002, **106**, 1380.
17 T. M. Reineke, M. Eddaoudi, M. Fehr, D. G. Kelley and O. M. Yaghi, *J. Am. Chem. Soc.*, 1999, **121**, 1651.
18 C. Serre, F. Millange, J. Marrot and G. Feréy, *Chem. Mater.*, 2002, **14**, 2409.
19 L. Pan, N. W. Zheng, Y. G. Wu, S. Han, R. Y. Yang, X. Y. Huang and J. Li, *Inorg. Chem.*, 2001, **40**, 828.
20 M. E. Braun, C. D. Steffek, J. Kim, P. G. Rasmussen and O. M. Yaghi, *Chem. Commun.*, 2001, 2532.
21 Z.-Y. Fu, X.-T. Wu, J.-C. Dai, S.-M. Hu, W.-X. Du, H.-H. Zhang and R.-Q. Sun, *Eur. J. Inorg. Chem.*, 2002, 2730.
22 H. Xu, N. Zheng, X. Jin, R. Yang and Z. Li, *Chem. Lett.*, 2002, 350.
23 Y. Wu, N. Zheng, R. Yang, H. Xu and E. Ye, *J. Mol. Struct.*, 2002, **610**, 181.
24 G. R. Desiraju, *Acc. Chem. Res.*, 1996, **29**, 441.
25 C. Sun, X. Zheng and L. Jin, *J. Mol. Struct.*, 2003, **646**, 201.
26 C. Janiak, *J. Chem. Soc., Dalton Trans.*, 2000, 3885.
27 L.-P. Zhang, Y.-H. Wan and L.-P. Jin, *J. Mol. Struct.*, 2003, **646**, 169.
28 G. M. Sheldrick, *SHELXL-97, Program for refinement of crystal structures*, University of Göttingen, Germany, 1997.
29 Y. Wan, L. Zhang, L. Jin, S. Gao and S. Lu, *Inorg. Chem.*, 2003, **42**, 4985.
30 H. Li, M. Eddaoudi, T. L. Groy and O. M. Yaghi, *J. Am. Chem. Soc.*, 1998, **120**, 8571.
31 J.-C. G. Bünzli, in *Lanthanide Probes in Life, Chemical and Earth Sciences. Theory and Practice*, ed. J.-C. G. Bünzli and G. R. Choppin, Elsevier, Amsterdam, 1989, ch. 7.
32 W. D. Horrocks and D. R. Sudnick, *Acc. Chem. Res.*, 1981, **14**, 384.
33 J. Tao, M.-L. Tong and X.-M. Chen, *J. Chem. Soc., Dalton Trans.*, 2000, 3669.